Appl. Phys. A 88, 611–615 (2007)
DOI: 10.1007/s00339-007-4076-8

Applied Physics A
Materials Science & Processing

J.X. WANG[1]
X.W. SUN[1,2,✉]
H. HUANG[1]
Y.C. LEE[1]
O.K. TAN[1]
M.B. YU[2]
G.Q. LO[2]
D.L. KWONG[2]

A two-step hydrothermally grown ZnO microtube array for CO gas sensing

[1] School of Electrical and Electronic Engineering, Nanyang Technological University, Nanyang Avenue, 639798 Singapore
[2] Institute of Microelectronics, 11 Science Park Road, Science Park II, Singapore 117685

Received: 24 January 2007 / Accepted: 19 April 2007
Published online: 7 June 2007 •

ABSTRACT Tubular ZnO microstructure arrays were fabricated on a large scale by a two-step hydrothermal method. The porous ZnO tubular structures were then used to construct a gas sensor for CO detection. The microtube array gas sensor showed sensitive response to different concentration of CO with an optimum temperature of 250 °C. Because of the large surface to volume ratio, the sensitivity of the microtube arrays was about twice of that of the ZnO rods. Our results indicate that this simple two-step method for fabrication of large-scale tubular microstructure arrays can be potentially used in gas sensor applications with improved performance.

PACS 81.07.Bc; 78.55.Et; 07.07.Df

1 Introduction

Semiconductor metal oxides have been widely used as gas sensing materials due to their advantages of low cost, high sensitivity and good compatibility with the fabrication process of silicon microelectronics [1]. ZnO, as a key semiconducting material, has been applied earlier in gas sensing for many toxic and hazard gases [2]. Since Seiyama et al. reported the gas sensor based on ZnO thin film in 1962 [3], many ZnO gas sensors have been developed [4, 5]. As the adsorption is a surface effect, the surface area is the most important parameter to determine the sensitivity of the gas sensor. However, the performance of traditional thin film gas sensor is severely hampered by the limited surface to volume ratio [6]. Though porous thin films have been adopted to enhance the surface area, oxide films with high porosity are difficult to synthesize [7]. In recent years, one-dimensional (1D) microstructures with a large surface to volume ratio have attracted much interest [8]. In fact, various oxide 1D structures such as nanowires [9, 10], nanoflower [11] and nanoflake [12] have been evaluated as gas sensors for the past few years.

Among various microstructures, tubular structures have attracted the extensive attention of researchers [13], due to their larger surface area and unique optical and electrical properties. Applications were extended to laser, medicine transport and transistor [13–16]. In addition, the hollow space inside the tube is advantageous in carrying functional materials to form complicated functional structures [17]. Though extensive efforts have been made to fabricate the tubular structures [18], large-scale synthesis of oxide tubular structures is still a challenge. In this letter, we shall report a two-step hydrothermal method to synthesis ZnO microtube arrays in large scale. The ZnO microtube array was used to construct a CO gas sensor with improved performance.

2 Experimental details

The synthesis of ZnO microtubes was carried out in a two-step hydrothermal method. In the first step, a 5 nm-thick ZnO thin film was firstly deposited on surface of a silicon (100) substrate with a thin SiO_2 layer, to facilitate the nucleation of ZnO nanorods in the hydrothermal process afterwards. The initial 5 nm ZnO film was fabricated by rf sputtering using a commercial Zn target (purity 99.99%). The power used for sputtering was 25 W. The base pressure was below 2×10^{-2} Pa. The growth time was 15 s and the Ar and O_2 gas flows were 40 and 2 sccm, respectively. Then ZnO nanorod array was synthesized on this ZnO-coated substrate. The aqueous hydrothermal solution consisting of 0.05 M $ZnCl_2$. $4H_2O$ and 0.05 M methenamine were mixed in a bottle with an auto-clavable screw cap, where a ten-minute sonication was carried out. Then the ZnO-coated silicon substrate was immersed vertically in the solution. The hydrothermal decomposition was carried out at 95 °C for 3 h inside an oven. After reaction, a white layer of products was seen deposited on the silicon substrate. In the second step, the as-prepared product was immersed in an ammonia solution (pH = 10.5) at 80 °C for 6 h. Then, the products were thoroughly washed with de-ionized water to remove the residual salts and amino complex. Subsequently, the morphology and structure were observed using scanning electron microscopy (SEM, JSM-6340F), X-ray diffraction (XRD, Siemens D5005) and high-resolution transmission electron microscopy (HRTEM, JEOL JEM-2010).

The gas sensing properties were characterized using a computer-controlled gas sensing characterization system. A pair of interdigital Au electrodes (1 mm gap between adjacent electrodes) with a thickness of 300 nm was deposited on the surface of the ZnO

✉ Fax: +65 6793 3318, E-mail: exwsun@ntu.edu.sg

microtube arrays by sputtering using a shadow mask. The testing gas was CO with various concentrations in dry air (relative humidity 30%). The gas sensitivity S was determined by the relative resistance, $S = I_{\text{gas}}/I_{\text{air}}$, where I_{air} and I_{gas} are the current of the ZnO microtube gas sensor in dry air and CO-containing dry air, respectively.

3 Results and discussion

Figure 1a shows the SEM image of the product synthesized in the first step. The inset of Fig. 1a is the corresponding cross-sectional SEM image. Rod-like structures with an average diameter of about 1 μm was found grown on the substrate. It can be seen also from the inset of Fig. 1a that the thin layer of ZnO underneath the rods becomes thicker (100–200 nm) compared to the initial thickness of 5 nm. Figure 1b–d show the planar-, titled- and enlarged-view SEM images of the as-prepared sample in the second step, respectively. The XRD data of the ZnO microtubes and rods arrays are shown in Fig. 2. All the diffraction peaks are in good agreement with the standard values for wurtzite ZnO (JCPDS 79-2205). The high intensity of (0002) peak in the XRD pattern of ZnO microrods indicates that the ZnO microrods array is preferentially oriented along (0002) direction. Compared to ZnO microrods array, the relative intensity of the (0002) peak of microtubes is low, which indicates absence of (000 n) planes in the hollow microtubes [19]. From the SEM images, we can see hexagonal ZnO tubular structures grow vertically on the substrate and form a dense array. The diagonal size of the hexagonal microtubes ranges from 200 nm to 2 μm with the average diameter of about 1 μm. The thickness of the wall of ZnO microtubes is about 100–200 nm, and the length of the microtubes is about 10 μm.

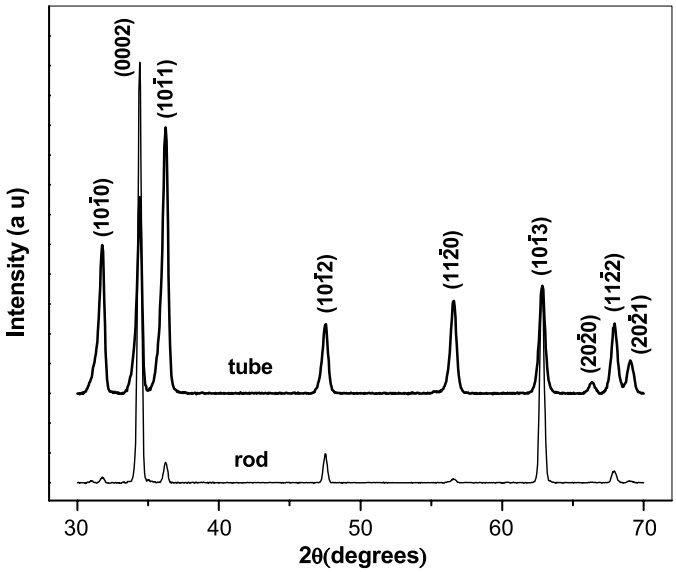

FIGURE 2 XRD pattern of ZnO microtubes array and ZnO microrods array

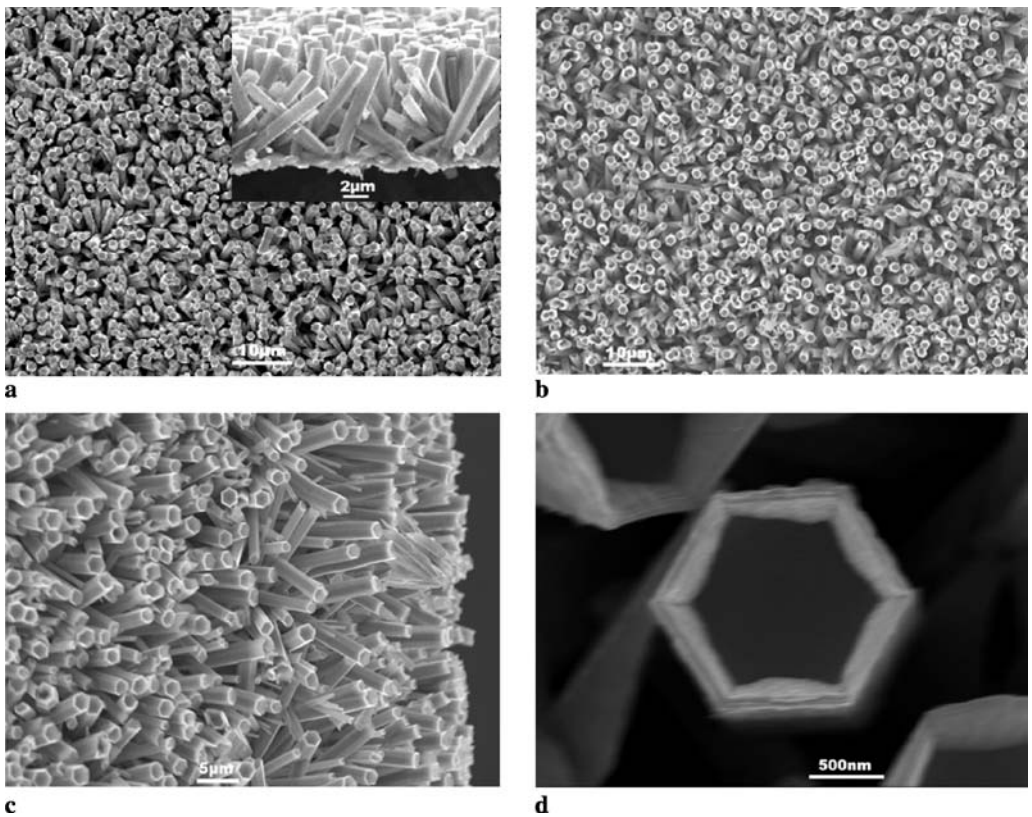

FIGURE 1 (**a**) SEM images of ZnO microrods array. (**b–d**) SEM images of ZnO microtubes array with the planar-, titled- and enlarged-view, respectively. The *inset* in (**a**) is the cross-section SEM image of the ZnO microrods array

Further insight into the detailed structure of the ZnO microtube was gained by TEM analysis. A typical TEM image of the microtube is shown in Fig. 3a. The inset of Fig. 3a is the corresponding select area electron diffraction (SAED) pattern. The sharp and bright dots in SAED pattern indicate that the microtubes is single crystalline. The growth direction of microtubes can be indexed to be [0001] direction. Figure 3b gives an HRTEM image taken at the top of the ZnO tube. The clear fringes correspond to the (0001) and $(01\bar{1}0)$ planes of hexagonal ZnO, respectively. HRTEM results further confirm the single crystalline feature of the ZnO tubes.

The growth mechanism of ZnO microtubes is discussed below. In the first step of synthesis process, Zn^{2+} ions and the NH_3^{2+} ion produced by dissolution of methenamine formed Zn^{2+} amino complex first, was then thermally decomposed to form ZnO rods [20, 21]. In the second step, the ZnO rods were immersed in the ammonia solution at the 80 °C. The hexagonal ZnO rod was confined by two (0001) plane and six $\{10\bar{1}0\}$ planes. Because of the higher concentration of NH_3^{2+} and lower temperature, the reaction moved in the reverse direction, and resulting in dissolution of ZnO [22]. It is well known that wurtzite ZnO is a polar crystal. The (0001) polar plane is metastable while the six nonpolar planes $\{10\bar{1}0\}$ are more stable. The fast growth direction [0001] is also the fast dissolution direction. Therefore, the preferential dissolution of ZnO (0001) plane finally resulted in the formation of hollow tubular structures along the [0001] direction.

Figure 4a shows the sensitivities of the ZnO microtubes [Fig. 1b] and microrods [Fig. 1a] gas sensors as a function of temperature exposed to a 250 ppm CO testing gas. The sensitivity of both ZnO tubes and rods increases initially with the increase of temperature reaching the maximum at 250 °C, and then decreases with further increase in temperature. However, the sensitivity of ZnO tubes is obviously higher than that of ZnO rods with almost the same diameter. The maximum sensitivity of microtubes at 250 °C, is about 2.1 times of that of rods, indicating the improved sensitivity of the ZnO tubes array. Based on the results shown in Fig. 4a, 250 °C was

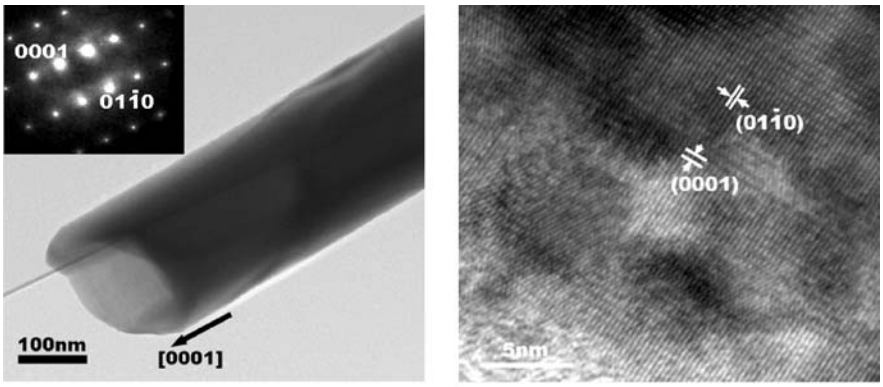

FIGURE 3 (**a**) A typical TEM image of the ZnO microtube, the *inset* is the corresponding SAED pattern. (**b**) HRTEM image of ZnO microtube taken on the tip of the microtube

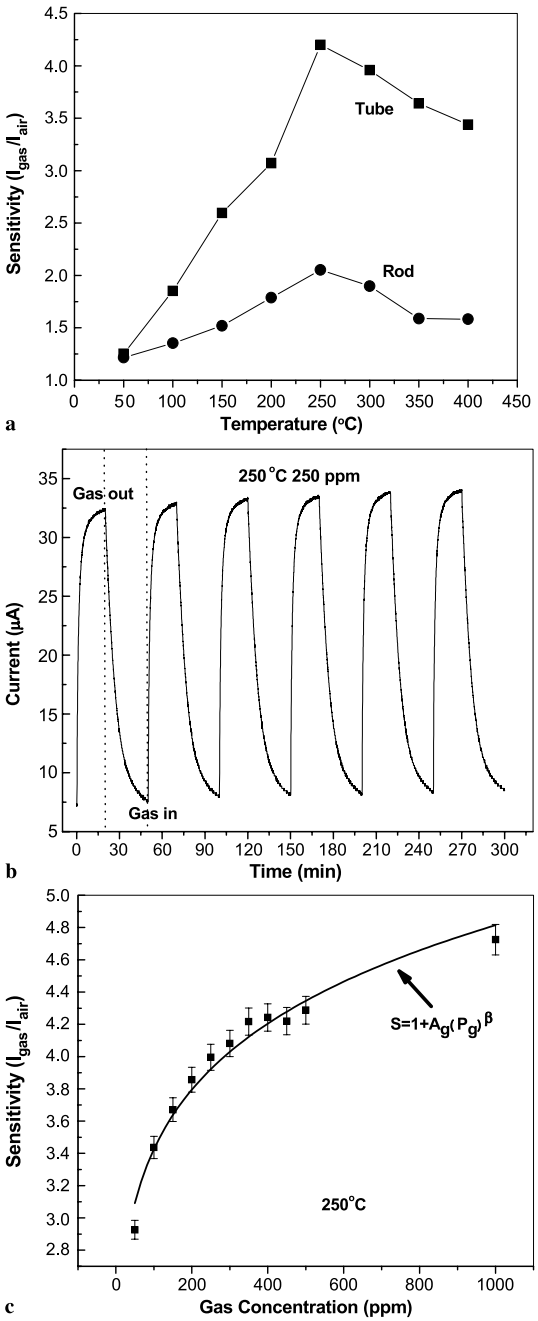

FIGURE 4 (**a**) The sensitivity of the ZnO microtubes and ZnO nanorods gas sensors as a function of temperature when the sensors were exposed to 250 ppm CO. (**b**) The response of ZnO microtubes gas sensor to 250 ppm CO at 250 °C. (**c**) The gas sensing performance of the ZnO microtubes in response to different concentration CO gas at temperature 250 °C

chosen to measure CO sensing properties of the ZnO microtube arrays. Figure 4b shows the switching response of ZnO microtube gas sensor to 250 ppm CO testing gas at 250 °C. The microtube gas sensor shows a reversible yet stable response to CO gas at this temperature. The conductivity of the ZnO sensor increases when it is exposed to CO and recovers to the baseline when the gas is turned off. The response time of the sensor to 250 ppm CO was estimated to be 54 s, indicating a fast response. Though the ZnO is reported not sensitive to CO gas as other oxides such as SnO_2 and In_2O_3 [6, 23], it is worth mentioning that the sensitivity of our ZnO tube sensor is significantly higher than that of the CO sensors constructed by ZnO films and ZnO nanoparticles [24–26].

It is also worth mentioning that, with a dense nanostructure (Fig. 1), the Au electrodes were able to form a continuous layer for gas sensing measurement. So the Au electrodes are not in direct contact the thin layer underneath the ZnO tube/rod array (inset of Fig. 1a). The current signal containing gas sensing information should pass through the ZnO tubes/rods, with tunneling in between them and possibly a small portion from the underlying ZnO thin layer connected to the tubes/rods. The different gas sensing responses from ZnO rods and tubes is a clear indication of this hypothesis.

Figure 4c shows the gas sensing performance of the ZnO microtubes in response to various concentrations CO testing gas at 250 °C. Following the increase of the gas concentration, the ZnO microtubes sensor shows an increasing response initially and saturates for higher CO concentration. Many models have been proposed to describe the sensing behavior of metal oxides [1]. When the process is mainly controlled by diffusion, the sensitivity of semiconducting oxide gas sensor can be empirically represented as $S = 1 + A_g(P_g)^{\beta}$, where P_g is the target gas partial pressure, which is proportional to the gas concentration, A_g is a prefactor, and β is the exponent on P_g [11, 27, 28]. Generally, β has an ideal value of either 0.5 or 1, which is derived from surface interaction between chemisorbed oxygen adions and reducing gas (CO, H_2) to the N-type semiconductors [27–29]. In our case, the value of β for microtubes array is about 0.197 ± 0.013, determined by the fit using the empirical formula. The deviation of the β may be due to the disorder and some insensitive area (vacancy between tubes) existing in the sensor [1, 27].

The sensing performance of semiconductor oxides is usually attributed to the adsorption and desorption of oxygen on the surface of the oxides [23, 29]. The absorbed oxygen captures free electrons and thus reducing the conductance of the oxide. When the oxides exposed to a reducing gas (CO in our case), the CO molecules react with the absorbed oxygen to form CO_2 molecules. This process causes the release of electrons from the oxygen ions, and thus increases the conductance. Figure 5 schematically depicts the sensing process of CO gas on the surface of a ZnO tube. The improved CO gas sensing performance of ZnO tubes over that of rod may be attribute to (1) the tubular structures improve the surface to volume ratio of the CO sensor and (2) the tubular structure form a real porous films that allow the gas molecules to diffuse deeply into the end of the film, thus exposing the so-called full surface of the microstructures to the testing gas.

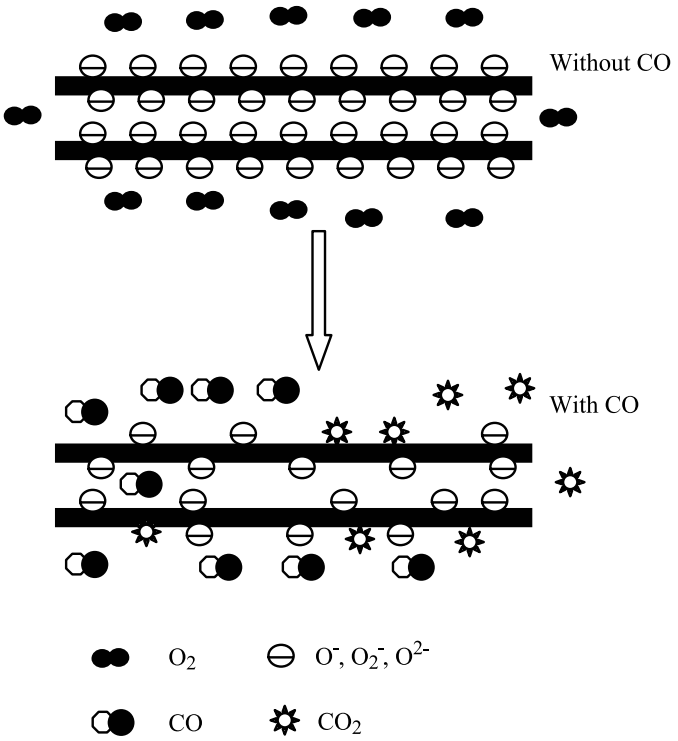

FIGURE 5 Schematic model of the CO sensing process of ZnO tube sensor

4 Conclusions

In summary, we have synthesized ordered tubular ZnO microstructure arrays using a simple two-step hydrothermal method. The tubular array was used to fabricate a CO gas sensor with improved sensitivity compared to rod array in a comparative study. Our two-step process is simple and can be easily scaled up for tubular microstructure arrays fabrication in large scale, which helps to realize various applications, for example the gas sensor shown here, with low costs.

ACKNOWLEDGEMENTS The sponsorships from Research Grant Manpower Fund (RGM 21/04) of Nanyang Technological University, and Science and Engineering Research Council Grant (#0421010010) and the Inter-RI ZnO Project from Agency for Science, Technology and Research (A*STAR), Singapore are gratefully acknowledged

REFERENCES

1 D.E. Williams, Sens. Actuators B **57**, 1 (1999)
2 H. Nanto, T. Minami, S. Takta, J. Appl. Phys. **60**, 482 (1986)
3 T. Seiyama, A. Kato, K. Fjishi, M. Nagatani, Anal. Chem. **34**, 1502 (1962)

4 S. Basu, A. Dutta, Sens. Actuators B **22**, 83 (1994)
5 T. Gao, T.H. Wang, Appl. Phys. A **80**, 1451 (2005)
6 C. Li, D.H. Zhang, B. Lei, S. Han, X.L. Liu, C.W. Zhou, J. Phys. Chem. B **107**, 12451 (2003)
7 G. Sberveglieri, G. Faglia, S. Groppelli, P. Nelli, Semicond. Sci. Technol. **5**, 1231 (1990)
8 Y. Xia, P. Yang, Y. Sun, Y. Wu, B. Mayers, B. Gates, Y. Yin, F. Kim, H. Yan, Adv. Mater. **15**, 353 (2003)
9 H.T. Wang, B.S. Kang, F. Ren, L.C. Tien, P.W. Sadik, D.P. Norton, S.J. Pearton, J. Lin, Appl. Phys. Lett. **86**, 243503 (2005)
10 J.X. Wang, X.W. Sun, Y. Yang, H. Huang, Y.C. Li, O.K. Tan, L. Vayssieres, Nanotechnology **17**, 4995 (2006)
11 Q. Wan, T.H. Wang, Chem. Commun. **30**, 3841 (2005)
12 Y. Liu, J. Dong, P.J. Hesketh, M.L. Liu, J. Mater. Chem. **15**, 2316 (2005)
13 M. Remskar, A. Mrzel, Z. Skraba, A. Jesih, M. Ceh, J. Demsar, P. Stadelmann, F. Levy, D. Mihailovic, Science **292**, 479 (2001)
14 D. Li, J.T. McCann, M. Marquez, Y. Xia, J. Am. Ceram. Soc. **89**, 1861 (2006)
15 X.W. Sun, S.F. Yu, C.X. Xu, C. Yuen, B.J. Chen, S. Li, Japan. J. Appl. Phys. **42**, L1229 (2003)
16 J. Goldberger, R. He, Y. Zhang, S. Lee, H. Yan, H.J. Choi, P. Yang, Nature **422**, 599 (2003)
17 J. Goldberger, R. Fan, P. Yang, Acc. Chem. Res. **39**, 239 (2006)
18 G.K. Mor, O.K. Varghese, M. Paulose, C.A. Grimes, Adv. Funct. Mater. **15**, 1291 (2005)
19 L. Vayssieres, K. Keis, A. Hagfeldt, S.E. Lindquist, Chem. Mater. **13**, 4395 (2001)
20 L. Vayssieres, K. Keis, S.E. Lindquist, A. Hagfeldt, J. Phys. Chem. B **105**, 3350 (2001)
21 L. Vayssieres, Int. J. Nanotechnol. **1**, 1 (2004)
22 A. Wei, X.W. Sun, C.X. Xu, Z.L. Dong, Y. Yang, S.T. Tan, W. Huang, Nanotechnology **17**, 1740 (2006)
23 H. Huang, O.K. Tan, Y.C. Lee, T.D. Tran, M.S. Tse, X. Yao, Appl. Phys. Lett. **87**, 163123 (2005)
24 H.W. Ryu, B.S. Park, S.A. Akbar, W.S. Lee, K.J. Hong, Y.J. Seo, D.C. Shin, J.S. Park, G.P. Choi, Sens. Actuators B **96**, 717 (2003)
25 H.Y. Bae, G.M. Choi, Sens. Actuators B **55**, 47 (1999)
26 H. Gong, J.Q. Hu, J.H. Wang, C.H. Ong, F.R. Zhu, Sens. Actuators B **115**, 247 (2006)
27 I.D. Kim, A. Rothschild, T. Hyodo, H.L. Tuller, Nano Lett. **6**, 193 (2006)
28 R.W.J. Scott, S.M. Yang, G. Chabanis, N. Coombs, D.E. Willams, G.A. Ozin, Adv. Mater. **13**, 1468 (2001)
29 A. Ponzoni, E. Comini, G. Sberveglieri, J. Zhou, S.Z. Deng, N.S. Xu, Y. Ding Z.L. Wang, Appl. Phys. Lett. **88**, 203101 (2006)